

## THE GROWTH OF THE STELLAR SEEDS OF SUPERMASSIVE BLACK HOLES

JARRETT L. JOHNSON<sup>1</sup>, DANIEL J. WHALEN<sup>2</sup>, CHRIS L. FRYER<sup>3</sup>, AND HUI LI<sup>1</sup>*Draft version December 3, 2024*

## ABSTRACT

The collapse of baryons into extremely massive stars with masses  $\gtrsim 10^4 M_\odot$  in a small fraction of protogalaxies at  $z \gtrsim 10$  is a promising candidate for the origin of supermassive black holes, some of which grow to a billion solar masses by  $z \sim 7$ . We determine the maximum masses such stars can attain by accreting primordial gas. We find that at relatively low accretion rates the strong ionizing radiation of these stars limits their masses to  $M_* \sim 10^3 M_\odot (\dot{M}_{\text{acc}}/10^{-3} M_\odot \text{ yr}^{-1})^{\frac{5}{7}}$ , where  $\dot{M}_{\text{acc}}$  is the rate at which the star gains mass. However, at the higher central infall rates usually found in numerical simulations of protogalactic collapse ( $\gtrsim 0.1 M_\odot \text{ yr}^{-1}$ ), the lifetime of the star instead limits its final mass to  $\gtrsim 10^6 M_\odot$ . Furthermore, for the spherical accretion rates at which the star can grow, its ionizing radiation is confined deep within the protogalaxy, so the evolution of the star is decoupled from that of its host galaxy. Ly $\alpha$  emission from the surrounding H II region is trapped in these heavy accretion flows and likely reprocessed into strong Balmer series emission, which may be observable by the *James Webb Space Telescope*. This, along with strong He II  $\lambda$  1640 and continuum emission, are likely to be the key observational signatures of the progenitors of supermassive black holes at high redshift.

*Subject headings:* stars: formation - accretion - ISM: H II regions - cosmology: early universe - theory - galaxies: formation

## 1. INTRODUCTION

The existence of  $10^8 - 10^9 M_\odot$  black holes (BH) in massive galaxies by  $z \sim 7$ , less than a billion years after the Big Bang (Fan et al. 2003; Willott et al. 2003; Mortlock et al. 2011), remains one of the great mysteries of cosmological structure formation. In the  $\Lambda$ CDM paradigm, early structure formation is hierarchical, with small dark matter halos at early epochs evolving into ever more massive ones by accretion and mergers through cosmic time. Hence, it is generally held that the supermassive black holes (SMBH) of the  $z \sim 7$  *Sloan Digital Sky Survey (SDSS)* quasars grow from much smaller seeds at high redshifts. The origin of these seeds, and how they reach such large masses by such early times, remains to be understood. Three main processes have been proposed for their formation (see Volonteri 2010): the collapse of Pop III stars into 100 - 300  $M_\odot$  BH at  $z \sim 20$  (e.g. Madau & Rees 2001; Alvarez et al. 2009; Milosavljević et al. 2009; Tanaka & Haiman 2009), the direct collapse of  $10^8 M_\odot$  dark matter halos that have somehow bypassed previous star formation into  $10^4 - 10^6 M_\odot$  BH at  $z \sim 10$  (e.g. Bromm & Loeb 2003; Koushiappas et al. 2004; Begelman et al. 2006; Lodato & Natarajan 2006; Spaans & Silk 2006; Omukai et al. 2008; Regan & Haehnelt 2009; Sethi et al. 2010; Inayoshi & Omukai 2011, see also Colgate et al. 2003), and the collapse of dense primeval star clusters into  $10^4 - 10^6 M_\odot$  BH (see e.g. Djorgovski et al. 2008; Devecchi & Volonteri 2009).

The processes by which black holes form at high redshift and evolve into SMBH must account for how they become so large by  $z \sim 7$  and why their numbers at that redshift are so small, about  $1 \text{ Gpc}^{-3}$ . Pop III seed BH are plentiful at  $z \sim 20 - 30$  but must grow at the Edington limit without interruption to reach  $10^8 - 10^9 M_\odot$

by  $z \sim 7$ . This is problematic because they and their progenitors either expel all the baryons from the shallow potential wells of the halos that create them, so they are "born starving" (Whalen et al. 2004; Johnson & Bromm 2007; Pelupessy et al. 2007; Alvarez et al. 2009; Jeon et al. 2011), or they eject themselves from their halos, and thus their fuel supply, at hundreds of km/s if they are born in core-collapse supernova explosions (Whalen & Fryer 2011 in prep). Also, accretion onto Pop III BH has been found to be inefficient on small scales, typically at most 20% Edington (Milosavljević et al. 2009; Park & Ricotti 2011), making the constant duty cycles required for sustained growth difficult (but see Li 2011).

If halos can instead congregate into primitive galaxies of  $\sim 10^8 M_\odot$  by  $z \sim 10 - 15$  without having first formed any stars, they reach virial temperatures of  $\sim 10^4 \text{ K}$  and begin to atomically cool. Numerical simulations of this process (Wise et al. 2008; Regan & Haehnelt 2009; Shang et al. 2010) find that in analogy to Pop III star formation in much smaller halos at higher redshifts (Nakamura & Umemura 2001; Bromm et al. 2002; Abel et al. 2002; O'Shea & Norman 2007; Yoshida et al. 2008; Turk et al. 2009; Stacy et al. 2010; Clark et al. 2011; Greif et al. 2011), baryons rapidly pool at the center of the halo and form a hydrostatic object. But this object is thought to become far more massive than Pop III stars modeled to date because atomic line cooling and the deeper potential well of the halo lead to much higher infall rates at its center,  $0.1 - 1 M_\odot \text{ yr}^{-1}$  rather than the  $10^{-4} M_\odot \text{ yr}^{-1}$  typical of primordial star-forming minihalos at  $z \sim 20$ . Such objects could collapse into black holes that are far more massive than Pop III BH (e.g. Shibata & Shapiro 2002), with Bondi-Hoyle accretion rates that allow them to grow into SMBH in less time (e.g.

<sup>1</sup> Nuclear and Particle Physics, Astrophysics and Cosmology Group (T-2), Los Alamos National Laboratory, Los Alamos, NM 87545; jlj@lanl.gov

<sup>2</sup> McWilliams Fellow, Department of Physics, Carnegie Mellon University, Pittsburgh, PA 15213

<sup>3</sup> CCS-2, Los Alamos National Laboratory, Los Alamos, NM 87545

Wyithe & Loeb 2011; but see Dotan et al. 2011).

One difficulty with this scenario is that it is not yet understood how primitive galaxies can form in the high Lyman-Werner UV backgrounds needed to fully quench Pop III star formation in its constituent halos prior to assembly (1 - 10 times those expected at the epoch of reionization at  $z \sim 6$ ; Dijkstra et al. 2008; Shang et al. 2010; Wolcott-Green et al. 2011, see also Agarwal et al. in prep). Furthermore, it is not known if the object at the center of the protogalaxy even becomes a star, because at such high accretion rates it reaches very large masses on timescales that are short in comparison to Kelvin-Helmholtz times and the onset of nuclear burning (although Ohkubo et al. 2009 have modeled the evolution of Pop III stars under accretion at much lower rates). It could be that the central object reaches such high entropies and densities that it is enveloped by an event horizon before reaching the main sequence (Fryer et al. 2001). If the central object becomes a star, what governs its rate of growth, its final mass, and thus the mass of the SMBH seed it becomes? Numerous authors have studied how stellar radiation regulates accretion onto Pop III protostars, but at much lower inflow rates than those in the centers of collapsing protogalaxies (e.g. Stahler et al. 1986; Omukai & Palla 2001; Omukai & Inutsuka 2002; McKee & Tan 2008; Stacy et al. 2011a; Hosokawa et al. 2011). Do the much higher accretion rates in primitive galaxies quench radiative feedback?

We have performed extensive semianalytical calculations of radiative feedback by Pop III supermassive stars in collapsing protogalaxies at  $z \sim 10$ . In §2, we examine the primary forms of radiative feedback on accretion onto the star (deferring the processes that can be ignored to thorough examination in the Appendix). We also derive the maximum mass that the supermassive star, and hence the SMBH seed, can achieve as a function of accretion rate, accounting for its prodigious ionizing UV flux. In §3, we estimate the maximum mass that the star can reach if it is limited by its finite lifetime rather than by radiative feedback. We discuss the observational signatures of rapidly accreting supermassive primordial stars in §4. Finally, in §5 we review the implications of final supermassive stellar mass for SMBH seed mass and the appearance of the first quasars in the Universe.

## 2. RADIATIVE FEEDBACK-LIMITED ACCRETION

We adopt an analytical approach to estimate the maximum mass that an accreting primordial star can ultimately attain in a collapsing  $10^7 - 10^8 M_\odot$  protogalaxy. For simplicity, we assume that accretion onto the star is constant and spherically-symmetric. We first consider the ionizing UV radiation emitted by the star, which is the dominant form of radiative feedback on the infall and envelops the star with an H II region. In particular, we make the following assumptions on the nature of the radiative feedback on the accretion flow (see Fig. 1):

(1) Outside the H II region, gas is accelerated only by gravity and falls inwards unchecked by gas or radiation pressure.

(2) Within the H II region, the gas is decelerated due to photoionization pressure only. This follows from the fact that the massive stars we consider here radiate at very

nearly the Eddington limit. By definition, this implies that the force due to electron scattering in the H II region exactly cancels that due to gravity; therefore, for simplicity we can assume that the only net force on the gas is due to photoionization pressure (see also Omukai & Inutsuka 2002).

In this Section we first determine how ionizing radiation from the supermassive star limits its growth via accretion. We then consider the effect of the Ly $\alpha$  photons to which the majority of the energy in the ionizing radiation is converted. We examine and exclude other processes that can contribute to feedback on accretion in the Appendix.

### 2.1. Suppression of Accretion by Photoionization

As we are considering constant, spherically-symmetric accretion, the equation that links the number density  $n$  of hydrogen nuclei and the velocity  $v$  of the gas at a distance  $r$  from the star is:

$$n(r) = \frac{\dot{M}_{\text{acc}}}{4\pi r^2 v(r) \mu m_{\text{H}}} . \quad (1)$$

Here, we assume that the gas is primordial with an average atomic weight of  $\mu m_{\text{H}} = 1.2 m_{\text{H}}$ , where  $m_{\text{H}}$  is the mass of the hydrogen atom.

Because the ionizing photons are trapped within the H II region, we assume that the velocity of the gas at its edge, at a distance  $r_{\text{HII}}$ , is just the free-fall velocity:

$$v(r_{\text{HII}}) = - \left( \frac{2GM_*}{r_{\text{HII}}} \right)^{\frac{1}{2}} . \quad (2)$$

We note that this velocity is much higher than the sound speed of the gas, at which infall is found to proceed from large radii in cosmological simulations (Wise et al. 2008; Shang et al. 2010; Johnson et al. 2011), so we neglect this small contribution to the gas velocity for simplicity.

The radius of the H II region,  $r_{\text{HII}}$ , is determined by the ionization front jump conditions, which require a balance between the rate  $Q$  at which ionizing photons are emitted from the star and the sum of the rate of hydrogen recombinations in the ionized volume (first term on the RHS in equation 3) and the rate at which neutral atoms enter the H II region through the accretion flow (second term on the RHS in equation 3). Following Raiter et al. (2010), we note that the rate at which ionizations occur is higher than  $Q$  by a factor  $P$  which accounts for corrections to the neutral hydrogen level populations at the high temperatures ( $\simeq 2-4 \times 10^4$  K; e.g. Whalen et al. 2004; Alvarez et al. 2006) expected for the H II regions of massive Pop III stars. To account for this rate, we take it that the total ionization rate in the H II region is  $Q_{\text{eff}} = PQ$ , where  $P$  is the ratio of the average ionizing photon energy and the ionization potential for neutral hydrogen, 13.6 eV. Integrating over the density profile of the gas in eq. 1 to find the radius at which the total number of recombinations in the enclosed volume balances the total number of photoionizations, we arrive at the following expression for  $r_{\text{HII}}$ :

$$\begin{aligned} Q_{\text{eff}} &\simeq \int_{r_*}^{r_{\text{HII}}} 4\pi \alpha_{\text{B}} r^2 n^2 dr + \frac{\dot{M}_{\text{acc}}}{\mu m_{\text{H}}} \\ &= \int_{r_*}^{r_{\text{HII}}} 4\pi \alpha_{\text{B}} r^2 \left[ \frac{\dot{M}_{\text{acc}}}{4\pi r^2 v(r) \mu m_{\text{H}}} \right]^2 dr + \frac{\dot{M}_{\text{acc}}}{\mu m_{\text{H}}} , \quad (3) \end{aligned}$$

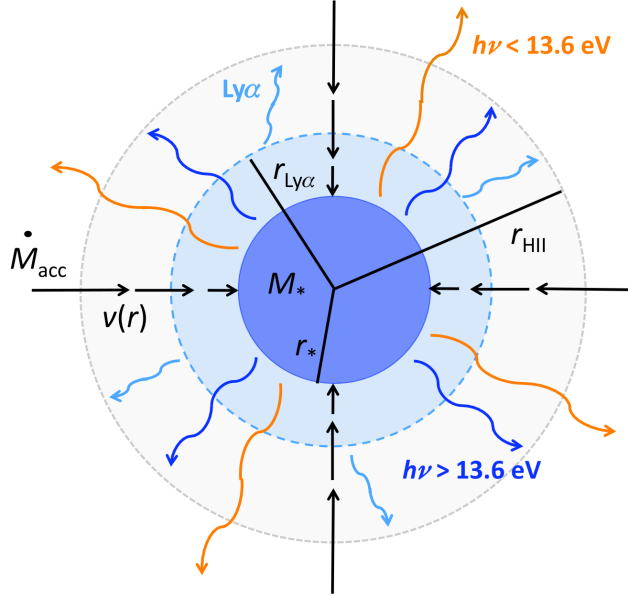


FIG. 1.— Schematic representation of accretion onto a supermassive Pop III star of mass  $M_*$  and radius  $r_*$ . Gas accretes at a constant rate  $\dot{M}_{\text{acc}}$ , being acted upon only by gravity at  $r > r_{\text{HII}}$ , the radius of the H II region of the star. Inside  $r_{\text{HII}}$  the gas, whose infall velocity is  $v(r)$ , is decelerated by momentum absorbed during ionizations, which is indicated by the shortening of the velocity vector arrows. While continuum photons with energies  $h\nu < 13.6$  eV escape the H II region and do not couple strongly to the gas even outside  $r_{\text{HII}}$ , resonant line photons do couple strongly and so in principle can also impart momentum to the gas. In particular, a large amount of momentum is emitted by H I recombinations as Ly $\alpha$ ; however, these photons couple so strongly to the gas that within  $r_{\text{Ly}\alpha}$  more than 50 percent of the emission is trapped in the accretion flow and cannot propagate outward and affect the dynamics of the flow. Within  $r_{\text{HII}}$ , Ly $\alpha$  photons are reprocessed into Balmer series photons which escape the H II region and may provide an observable signature of accreting supermassive stars (see § 4).

where  $\alpha_{\text{B}} \simeq 1.4 \times 10^{-13} \text{ cm}^3 \text{ s}^{-1}$  is the recombination coefficient for  $\gtrsim 2 \times 10^4$  K photoionized primordial gas (Whalen et al. 2004; Osterbrock & Ferland 2006). Following Omukai & Inutsuka (2002), for simplicity we neglect the second term in our calculations, as it is in general much smaller than  $Q_{\text{eff}}$ . This is true in particular for the solutions that we find for the minimum accretion rate onto a star of a given mass; at much higher rates, this term may become large, likely limiting the radius of the H II region.

Finally, once the accreting gas crosses the stationary ionization front (as shown in Fig. 1), the equation that governs its deceleration due to momentum imparted by photoionizations is:

$$v \frac{dv}{dr} = -\frac{\alpha_{\text{B}} h\nu n}{\mu m_{\text{H}} c} = -\frac{\alpha_{\text{B}} h\nu}{\mu m_{\text{H}} c} \left[ \frac{\dot{M}_{\text{acc}}}{4\pi r^2 v(r) \mu m_{\text{H}}} \right], \quad (4)$$

where again we have assumed that the photoionization rate of hydrogen is balanced its recombination rate,  $\alpha_{\text{B}} n$ , and that the momentum transferred to the gas per photoionization is  $h\nu/c$ . For the massive primordial stars that we consider here, we take the effective surface temperature of the star to always be  $\simeq 10^5$  K, which yields an average energy per ionizing photon  $h\nu \simeq 29$  eV. In turn, this implies  $P \equiv h\nu/13.6 \text{ eV} = 2.1$ , which we assume throughout our study. In equation (4) we again choose case B, as we assume that recombinations to the ground level of hydrogen result in the emission of photons which do not deposit a net momentum to the gas (being emitted isotropically and contributing to the diffuse radiation field).<sup>4</sup>

To find the solutions for steady state accretion, we must solve the equation of motion equation 4. In particular, to find the minimum accretion rate for which an inflow solution exists, we search for solutions for which the infall velocity of the gas goes to zero at the stellar surface  $r_*$ :

$$v(r_*) = 0. \quad (5)$$

That is, we must simultaneously solve equations 3 and 4, under the constraints given by equations 2 and 5. These constraints yield the maximum mass that the star can achieve by steady accretion before its intense ionizing radiation halts infall at  $r > r_*$  and prevents its further growth. On the other hand, they also yield the lower bound for the final mass of the central object, since for  $v(r_*) > 0$  radiative feedback fails to cut off accretion and the star will grow even faster than when gas merely comes to a halt on its surface.

The solution to equation 4 has the general form

$$v(r) = \left[ \left( \frac{3\alpha_{\text{B}} h\nu \dot{M}_{\text{acc}}}{4\pi \mu^2 m_{\text{H}}^2 c} \right) r^{-1} - K \right]^{\frac{1}{3}}, \quad (6)$$

where  $K$  is a constant whose value must satisfy the constraint that  $v(r_*) = 0$ . This yields for  $K$

$$K = \left( \frac{3\alpha_{\text{B}} h\nu \dot{M}_{\text{acc}}}{4\pi \mu^2 m_{\text{H}}^2 c} \right) r_*^{-1}. \quad (7)$$

The equation for the infall velocity in the H II region then becomes

<sup>4</sup> At the high densities in the H II regions we consider (Fig. 2) and with the enhanced population of neutral hydrogen in the  $n = 2$  state due high temperatures in primordial H II regions (Raiter et al. 2010), a  $\sim 30$  percent smaller 'extended case B' (Hummer & Storey 1987) recombination coefficient may be more appropriate, but our final results are not strongly dependent on this choice.

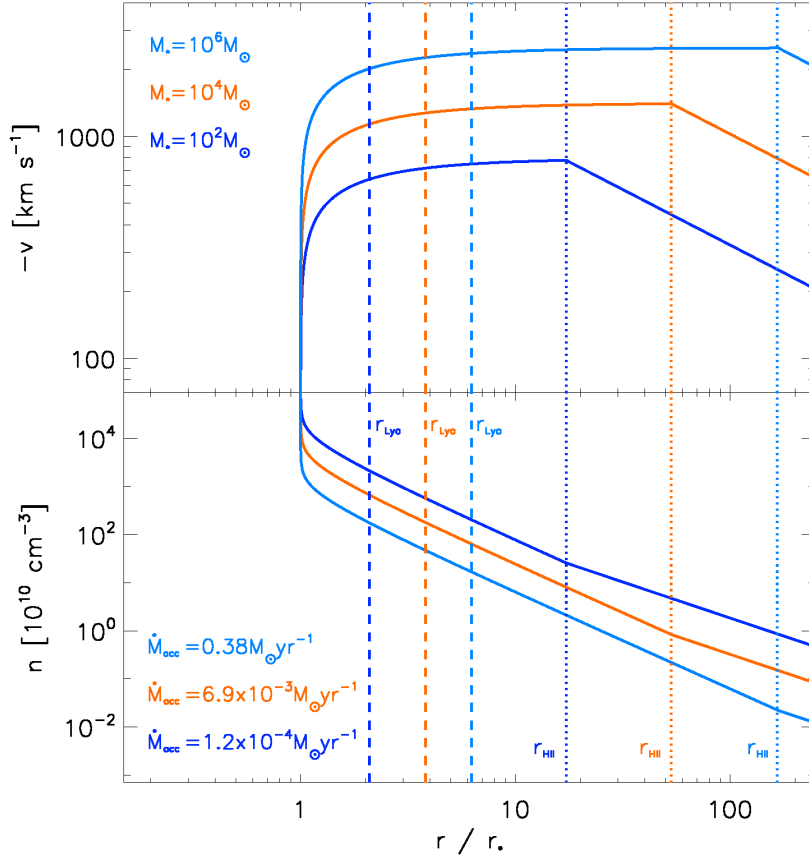


FIG. 2.— The infall velocity (*top panel*) and density (*bottom panel*) of the gas accreting onto primordial stars as a function of distance  $r$  from the center of the star for three stellar masses:  $10^2$  (*dark blue*),  $10^4$  (*red*), and  $10^6 M_\odot$  (*light blue*). Each star accretes at the minimum rate (as labeled) its strong ionizing flux permits, as given by equation 11. The dotted lines show the radius  $r_{\text{HII}}$  of the H II regions surrounding the stars, with their colors corresponding to those of the respective stellar masses. Outside the H II region, the gas is in free-fall, but after crossing into the H II region boundary it is rapidly photoionized and decelerated until it arrives at the stellar surface with velocity  $v(r_*) = 0$ . The dashed lines show the trapping radius  $r_{\text{Ly}\alpha}$  for Ly $\alpha$  photons from recombinations in the H II region (assuming a gas temperature of  $4 \times 10^4$  K, see equation 22); partly because the vast majority of these photons are trapped within  $r_{\text{Ly}\alpha}$ , we can neglect Ly $\alpha$  scattering feedback as discussed in §2.2. Accretion at rates below those shown here is not possible, as in such cases  $r_{\text{HII}} \rightarrow \infty$  and photoionization pressure halts infall at all radii.

$$v(r) = \left[ \left( \frac{3\alpha_{\text{B}} h\nu \dot{M}_{\text{acc}}}{4\pi\mu^2 m_{\text{H}}^2 c} \right) r^{-1} - \left( \frac{3\alpha_{\text{B}} h\nu \dot{M}_{\text{acc}}}{4\pi\mu^2 m_{\text{H}}^2 c} \right) r_*^{-1} \right]^{\frac{1}{3}}. \quad (8)$$

As shown in Figure 2, these solutions give a relatively constant velocity for the gas in the H II region until it is very close to the stellar surface. In turn, equation (1) implies that  $n(r)$  is essentially  $\propto r^{-2}$  in the H II region.

Applying this  $v(r)$  (and hence  $n(r)$ ) to the integral in equation 3 and evaluating it yields  $r_{\text{HII}}$ :

$$r_{\text{HII}} = \left[ r_*^{-1} - \frac{4\pi Q_{\text{eff}}^3}{3\alpha_{\text{B}}} \left( \frac{h\nu\mu m_{\text{H}}}{c} \right)^2 \dot{M}_{\text{acc}}^{-4} \right]^{-1}. \quad (9)$$

Finally, we must satisfy the constraint given by equation 2 to find the solution for the minimum accretion rate. Substituting equations 8 and 9 into equation 2 and rearranging the terms gives the following quadratic equation in  $\dot{M}_{\text{acc}}^2$ :

$$0 = \left( \frac{2GM_*}{r_*} \right) \dot{M}_{\text{acc}}^4 - \left( \frac{Q_{\text{eff}} h\nu}{c} \right)^2 \dot{M}_{\text{acc}}^2 - \frac{8\pi GM_* Q_{\text{eff}}^3}{3\alpha_{\text{B}}} \left( \frac{h\nu\mu m_{\text{H}}}{c} \right)^2, \quad (10)$$

whose solution is

$$\dot{M}_{\text{acc}}^2 = \frac{\left( \frac{Q_{\text{eff}} h\nu}{c} \right)^2 + \left[ \left( \frac{Q_{\text{eff}} h\nu}{c} \right)^4 + \frac{64\pi Q_{\text{eff}}^3}{3\alpha_{\text{B}} r_*} \left( \frac{GM_* h\nu\mu m_{\text{H}}}{c} \right)^2 \right]^{\frac{1}{2}}}{\frac{4GM_*}{r_*}}. \quad (11)$$

Noting that the second term in the square brackets is much larger than the first, we have

$$\dot{M}_{\text{acc}} \simeq \left( \frac{4\pi Q_{\text{eff}}^3 r_*}{3\alpha_{\text{B}}} \left( \frac{h\nu\mu m_{\text{H}}}{c} \right)^2 \right)^{\frac{1}{4}}, \quad (12)$$

<sup>5</sup> While in our solution the H II region formally extends to infinity in this case, for accretion to be terminated it need only extend to the Bondi radius, outside of which gas cannot be gravitationally captured by the star.

which exactly matches the accretion rate for which the H II region breaks out to infinity (see equation 9) and therefore stops accretion entirely because photoionization pressure exerts a net outward force on gas at all radii.<sup>5</sup> Thus, we see that the H II region is confined and that accretion proceeds at infall rates higher than those given by equation 12 and that no inflow solutions exist for lower rates.<sup>6</sup>

Now, by expressing  $Q$  ( $= Q_{\text{eff}} = PQ$ , where  $P = 2.1$ ) and  $r_*$  just in terms of the stellar mass  $M_*$ , we can find the maximum stellar mass for which accretion onto the star is permitted (at  $\dot{M}_{\text{acc}}$  in equation 12). We can take it that, if the star is thermally relaxed<sup>7</sup> and radiating at the Eddington limit (Begelman 2010), then the following two equations relate the mass  $M_*$  of the star to its ionizing photon emission rate  $Q$  and radius  $r_*$ :

$$Q = 1.6 \times 10^{50} \text{ s}^{-1} \left( \frac{M_*}{100 M_\odot} \right), \quad (13)$$

and

$$r_* = 3.7 R_\odot \left( \frac{M_*}{100 M_\odot} \right)^{\frac{1}{2}}. \quad (14)$$

These are from Table 1 of Bromm et al. (2001) and are in good agreement with Schaerer (2002) and Begelman (2010). With these expressions, we find that the solution to equation 12 is

$$M_* \simeq 10^3 M_\odot \left( \frac{\dot{M}_{\text{acc}}}{10^{-3} M_\odot \text{ yr}^{-1}} \right)^{\frac{8}{7}}, \quad (15)$$

where  $M_*$  is the maximum stellar mass attainable under accretion of gas at a rate  $\dot{M}_{\text{acc}}$ .

We plot this maximum stellar mass in Figure 3. As we shall see, the feedback due to ionizing radiation emitted by the star can limit its mass at relatively low accretion rates, which we term 'feedback-limited accretion'. However, at higher accretion rates the finite lifetime of the star governs its maximum mass; we term this 'time-limited accretion'. We discuss why this is so in §3.

Although we have focused on the pressure due to hydrogen photoionizations, it is straightforward to include He I photoionizations under the condition that within the H II region He I is also photoionized to He II. For the relatively hard spectra of massive primordial stars this is a sound assumption because the number of He I-ionizing photons is comparable to the number of H I-ionizing photons (Schaerer 2002). The ratio of the radiation pressures from helium and hydrogen photoionization is then

$$\frac{p_{\text{HeI}}}{p_{\text{HI}}} \simeq \frac{n_{\text{He}}}{n_{\text{H}}} \frac{h\nu_{\text{HeI}}}{h\nu_{\text{HI}}} \frac{\alpha_{\text{B,HeI}}}{\alpha_{\text{B,HI}}} \simeq 0.14, \quad (16)$$

where the first term is the ratio of helium and hydrogen number densities, which is  $\simeq 0.1$ . The second term is the ratio of the average ionizing photon energies for He I and

H I, which by integrating the stellar spectrum of a  $10^5$  K primordial star we find to be  $38 \text{ eV}/29 \text{ eV} \simeq 1.3$ . The third term is the ratio of He I and H I case B recombination coefficients, which is  $\simeq 1.1$  (Osterbrock & Ferland 2006). While this is a relatively modest increase in the radiation pressure, for completeness we include it as a multiplicative coefficient when solving equation 4. Other forms of radiation pressure are not so easily accommodated by our analytical approach but can be neglected without strongly affecting our conclusions, as we discuss in the next Section and in the Appendix.

## 2.2. Trapping of Ly $\alpha$ photons

In the H II region of the accreting star, a large fraction of the ionizing radiation is reprocessed into Lyman  $\alpha$  photons, which couple very strongly to primordial gas and could impart significant momentum to it, as they in principle can scatter many times across the H II region (Oh & Haiman 2002; McKee & Tan 2008). We can estimate how Lyman  $\alpha$  photons inhibit accretion by comparing their momentum to the momentum of the accretion flow. The former is given by (Raiter et al. 2010)

$$\frac{L_{\text{Ly}\alpha}}{c} \simeq \beta_{\text{Ly}\alpha} h\nu_{\text{Ly}\alpha} \frac{Q_{\text{eff}}}{c} \simeq 10^{29} \text{ g cm s}^{-2} \left( \frac{M_*}{100 M_\odot} \right), \quad (17)$$

where  $L_{\text{Ly}\alpha}$  is the Ly $\alpha$  luminosity due to recombinations in the H II region, in which  $\beta_{\text{Ly}\alpha}$  ( $\simeq 0.9$ ) Ly $\alpha$  photons, each with an energy  $h\nu_{\text{Ly}\alpha} = 1.6 \times 10^{-11}$  erg, are emitted for every recombination (Osterbrock & Ferland 2006; Raiter et al. 2010).<sup>8</sup> Here, we have also related the number of ionizing photons emitted per second  $Q$  to the stellar mass  $M_*$  with equation 13. The momentum of the accretion flow is

$$\dot{M}_{\text{acc}} v \simeq 6 \times 10^{33} \text{ g cm s}^{-2} \left( \frac{v}{10^3 \text{ km s}^{-1}} \right) \left( \frac{\dot{M}_{\text{acc}}}{M_\odot \text{ yr}^{-1}} \right), \quad (18)$$

where we have normalized the infall velocity  $v$  to its typical value at the edge of the H II region in the solutions shown in Fig. 2, since this is where Lyman  $\alpha$  photons will be most strongly coupled to the gas (indeed, these photons are trapped within the accretion flow at  $r_{\text{HII}}$ , as shown below). Equating these two expressions and using the relation between  $\dot{M}_{\text{acc}}$  and  $M_{*,\text{max}}$  in equation 15, we find the conditions under which Lyman  $\alpha$  radiation pressure could halt accretion:

$$v \lesssim 600 \text{ km s}^{-1} \left( \frac{\dot{M}_{\text{acc}}}{0.1 M_\odot \text{ yr}^{-1}} \right)^{\frac{1}{7}}. \quad (19)$$

Since the inflow velocity near the edge of the H II region is well above this value at the typical minimum accretion rates we find ( $\lesssim 0.1 M_\odot \text{ yr}^{-1}$ ; see Fig. 2), it is clear that Lyman  $\alpha$  radiation pressure has only a small impact on accretion in comparison to photoionization pressure. In

<sup>6</sup> Relatively small deviations from the solutions we have found for  $v(r)$  at  $r_{\text{HII}}$  may result in a shock developing there. However, even for a strong shock for which there is a density jump of a factor of four, the minimum accretion rates in equation 11 change by  $\lesssim 20$  percent.

<sup>7</sup> At the minimum accretion rates we find for a given stellar mass (e.g. equation 15), the 'trapping' radius due to electron scattering (which is proportional to the accretion rate, e.g. Begelman 1978) is always smaller than the stellar radius given by equation 14. Therefore, the main sequence stars we consider here are thermally relaxed (see also Ohkubo et al. 2009). At higher accretion rates, the radiation emitted by the star can become trapped due to electron scattering, resulting in an expansion of the stellar photosphere (see Omukai & Palla 2003, for a discussion of this effect on primordial protostellar growth).

<sup>8</sup> We note that in the high densities in the H II regions we consider (see Fig. 2), frequent collisions can prevent the radiative decay of hydrogen via two photon emission, which raises the Ly $\alpha$  luminosity above that expected in the low density regime, where  $\beta_{\text{Ly}\alpha} \simeq 0.68$  (Spitzer 1978).

particular, over the range of stellar masses and critical accretion rates that we consider (Figs. 2 and 3), we find that the infall velocity is  $\sim$  three times that in equation 19. In other words, at the high accretion rates we find, the momentum of inflow is always roughly three times what could be countered by Ly $\alpha$  scattering.

It might be thought that if a Lyman  $\alpha$  photon is scattered and then traverses the H II region, it could subsequently be scattered many times, thereby enhancing the momentum it imparts the gas (see Adams 1972; Milosavljević et al. 2009). However, upon scattering from an atom in the rapid ( $\simeq 10^3$  km s $^{-1}$ ) accretion flow, the photon would be strongly blue-shifted relative to the gas entering the opposite side of the H II region; as a result, it would couple to gas much less strongly thereafter, greatly limiting the degree to which it could add more momentum to the gas (see Dijkstra & Wyithe 2010, on how galactic outflows enhance Ly $\alpha$  escape by this process).

Furthermore, another effect which dramatically lessens the impact of Ly $\alpha$  photons on accretion is that their large resonant scattering cross section ensures that they are trapped in the H II region and do not scatter out to larger radii. To see this, we follow Begelman (1978) in defining the trapping radius for Ly $\alpha$ :

$$r_{\text{Ly}\alpha} \simeq 5 \times 10^{24} \text{ cm} \left( \frac{\dot{M}_{\text{acc}}}{M_{\odot} \text{ yr}^{-1}} \right) f_{\text{HI}} \left( \frac{T}{10^4 \text{ K}} \right)^{-\frac{1}{2}}, \quad (20)$$

where  $f_{\text{HI}}$  is the neutral hydrogen fraction,  $T$  is the temperature of the ionized gas, and we have used  $\sigma_{\text{Ly}\alpha} = 5.9 \times 10^{-14} \text{ cm}^2 (T/10^4 \text{ K})^{-\frac{1}{2}}$  for the cross section for Lyman  $\alpha$  scattering (Milosavljević et al. 2009). The fraction of neutral hydrogen in the H II region can be estimated by assuming photoionization equilibrium<sup>9</sup>; we obtain

$$\begin{aligned} f_{\text{HI}} &\simeq \frac{4\pi\alpha_{\text{B}}n(r)r^2}{Q_{\text{eff}}\sigma_{\text{HI}}} \\ &= 3 \times 10^{-5} \left( \frac{n}{10^{10} \text{ cm}^{-3}} \right) \left( \frac{r}{10^{15} \text{ cm}} \right)^2 \left( \frac{Q_{\text{eff}}}{10^{50} \text{ s}^{-1}} \right)^{-1} \end{aligned} \quad (21)$$

where  $\sigma_{\text{HI}} = 6 \times 10^{-18} \text{ cm}^2$  is the photoionization cross section for H I (although it is likely slightly lower due to the relatively hard spectrum of the star; see e.g. Johnson & Khochfar 2011). Then with this  $f_{\text{HI}}$ ,  $Q$  from equation 13,  $n(r)$  from equation 1, and  $\dot{M}_{\text{acc}}$  in terms of  $M_*$  from equation 15, we find:

$$\begin{aligned} r_{\text{Ly}\alpha} &\simeq 10^{12} \text{ cm} \left( \frac{M_*}{100 M_{\odot}} \right)^{\frac{3}{4}} \\ &\times \left( \frac{v}{10^3 \text{ km s}^{-1}} \right)^{-1} \left( \frac{T}{10^4 \text{ K}} \right)^{-\frac{1}{2}}. \end{aligned} \quad (22)$$

Assuming a temperature of  $4 \times 10^4$  K for the photoionized primordial gas (Whalen et al. 2004; Kitayama et al. 2004), Ly $\alpha$  trapping radii for three cases are shown in Fig. 2. We see that  $r_{\text{Ly}\alpha}$  is  $\sim 2 - 6 r_*$  and is smaller than  $r_{\text{HII}}$  by roughly an order of magnitude. While this is a modest

fraction of the volume of the H II region, because of its steep density profile ( $n \propto r^{-2}$ ) most of the Ly $\alpha$  photons originate from this region.

Integration of equation 3 shows that the fraction of recombinations produced in the H II region as a function of  $r$  is  $\sim (r_*^{-1} - r^{-1}) / (r_*^{-1} - r_{\text{HII}}^{-1})$ . Consequently, the fraction of Ly $\alpha$  photons originating from within the trapping radius is  $(r_*^{-1} - r_{\text{Ly}\alpha}^{-1}) / (r_*^{-1} - r_{\text{HII}}^{-1})$ , or  $\gtrsim 0.5$ . Thus, most of them are trapped deep in the H II region and cannot propagate outward to slow accretion at greater radii. Ly $\alpha$  scattering thus removes only  $\sim 15\%$  of the momentum of infall, not 30%, so we are justified in neglecting its impact on accretion flow.

At this point, we can show that Ly $\alpha$  photons created outside  $r_{\text{Ly}\alpha}$  but within  $r_{\text{HII}}$  are also trapped in the accretion flow at the boundary of the H II region due to the huge optical depth of the neutral gas to these photons. This is easily shown by equation 20, which for a largely neutral medium (i.e.  $f_{\text{HI}} \simeq 1$ ) yields a trapping radius on the order of  $10^{21}$  cm for the lowest accretion rates given by our solution (equation 12); as this is much larger than both  $r_{\text{HII}}$  and the Bondi radius, the maximum distance from which the protogalactic gas in can accrete onto the star.<sup>10</sup> Therefore, we can also safely conclude that Ly $\alpha$  photons will not escape from the H II region to affect the dynamics of the accretion flow at larger radii.

We note that although Ly $\alpha$  is trapped deep in the H II region, the thermal state of the gas may not be greatly affected because cooling via other atomic transitions in hydrogen still occurs (see e.g. Raiter et al. 2010; Schleicher et al. 2010). As shown by Schleicher et al. (2010), trapped Ly $\alpha$  photons boost the populations of both the H(2s) and the H(3) states of H, radiative decay from which results in the emission of photons that exit the H II region. Thus, photoionization heating of the gas is still balanced by efficient radiative cooling, so even though much of the stellar radiation is reprocessed in the H II region it still eventually emerges and may be observable (see § 4).<sup>11</sup> It follows that the luminosity of the outgoing radiation is always the same as that of the star; since the star is taken to shine at the Eddington limit, this in turn implies that the force due to electron scattering indeed balances the force due to gravity everywhere in the highly ionized H II region, as we assumed in our calculation. It follows that the temperature of the gas is low enough to keep the flow supersonic so gas pressure cannot stop accretion, as we discuss in the Appendix. Overall, we conclude that ionizing photons, despite mostly being converted to Ly $\alpha$  photons, are what primarily regulate the growth of supermassive primordial stars.

### 3. TIME-LIMITED ACCRETION

As noted by Begelman (2010), the lifetime of a very massive primordial star burning nuclear fuel at the Eddington rate  $L_{\text{Edd}}$  and growing by accretion at a constant rate is  $t_{\text{life}} \simeq 4$  Myr, twice the lifetime of non-accreting Pop III

<sup>9</sup> Comparing the rates of hydrogen photoionization and collisional ionization using the rate given by Cen (1992), we find that the former is much greater than the latter; thus, photoionization equilibrium is a valid assumption.

<sup>10</sup> The Bondi radius is roughly  $r_{\text{Bondi}} \simeq 10^{16} (M_*/100 M_{\odot}) \text{ cm}$ , assuming a sound speed in the protogalactic gas of  $10 \text{ km s}^{-1}$ , following Wise et al. (2008) and Shang et al. (2010).

<sup>11</sup> To be precise, for a star with an effective temperature of  $10^5$  K, roughly 60 percent of its luminosity is emitted in ionizing photons, which are later reprocessed into nebular continuum and recombination emission, such as Ly $\alpha$ .

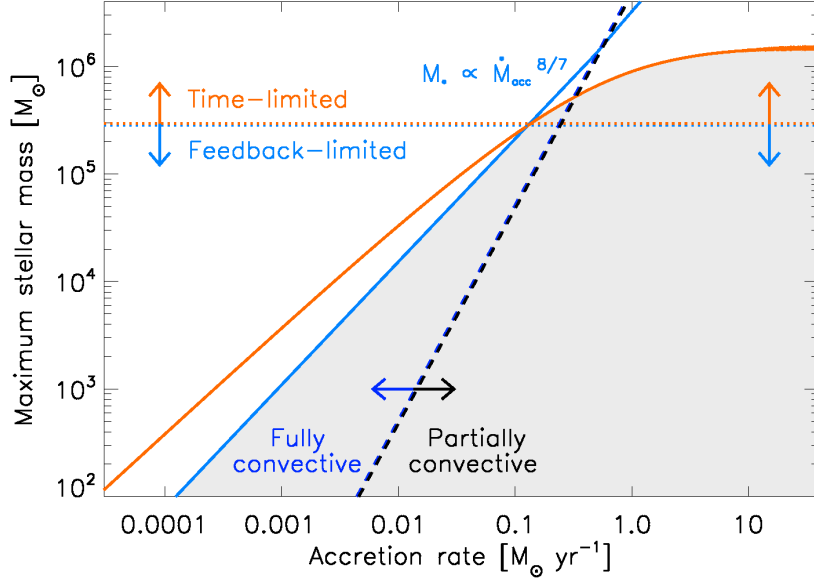


FIG. 3.— The maximum mass to which a star can grow at a constant accretion rate  $\dot{M}_{\text{acc}}$ . Above the maximum mass  $M_* \propto \dot{M}_{\text{acc}}^{8/7}$  given by equation 15 (*blue line*), radiative feedback shuts off accretion because the H II region of the star breaks out and prevents gas infall. For accretion rates  $\gtrsim 10^{-1} M_{\odot} \text{ yr}^{-1}$ , the maximum mass is set instead by the lifetime of the star (*red line*). While at relatively low accretion rates the lifetime of an accreting massive primordial star is  $\sim 4$  Myr, at high accretion rates the stellar lifetime can be shortened dramatically due to the super-Eddington luminosity at which nuclear fuel must be burned to support it during its growth. Also, at high accretion rates (right of the dashed curve), the star ceases to be fully convective and only the material in the convective core of the star is available for nuclear burning, further limiting the lifetime of the supermassive star. As the red curve shows, together these factors lead to a maximum stellar mass, for even the highest accretion rates, of  $\sim 1.5 \times 10^6 M_{\odot}$ . The dotted horizontal line delineates the mass ( $\sim 3 \times 10^5 M_{\odot}$ ) above which the final mass of a star is dictated by the limited time available for growth and below which it is governed by radiative feedback. The shaded area denotes the range of possible stellar masses for accretion at a constant rate.

stars of similar mass.<sup>12</sup> However, the stellar lifetime is in fact shorter than this for two reasons. First, nuclear fuel must be burned at a higher rate than the Eddington limit to support the star against its constantly increasing mass. Thus, the star consumes fuel at the rate (Begelman 2010)

$$L_{\text{nuc}} = L_{\text{Edd}} + \frac{GM_* \dot{M}_{\text{acc}}}{r_*} = L_{\text{Edd}} \left( 1 + \frac{r_{\text{trap}}}{r_*} \right), \quad (23)$$

where  $r_*$  is the radius of the star (equation 14),  $r_{\text{trap}} = 6 \times 10^{13} \text{ cm}$  ( $\dot{M}_{\text{acc}}/M_{\odot} \text{ yr}^{-1}$ ) is the radius at which radiation is trapped in the accretion flow by electron scattering, and  $L_{\text{Edd}} = 1.2 \times 10^{40} \text{ erg s}^{-1}$  ( $M_*/100 M_{\odot}$ ) is the Eddington rate for a star of mass  $M_*$ .

Second, for accretion rates above  $\dot{M}_{\text{acc,trap}} \simeq 4.3 \times 10^{-3} M_{\odot} \text{ yr}^{-1}$  ( $M_*/100 M_{\odot}$ )<sup>1/2</sup> radiation is trapped above the surface of the star and its envelope ceases to be convective (Begelman 2010).<sup>13</sup> This limits the fuel supply of the star to the mass within its convective core, whose fraction of the total mass is (equation 26 of Begelman 2010)

$$\frac{M_{\text{conv}}}{M_*} \simeq 0.54 \left( \frac{r_{\text{trap}}}{r_*} \right)^{2/3} \left( \frac{\dot{M}_{\text{acc}}}{M_{\odot} \text{ yr}^{-1}} \right)^{-2/3} \left( \frac{M_*}{10^6 M_{\odot}} \right)^{1/3}, \quad (24)$$

where we have assumed a central temperature of  $10^8 \text{ K}$ .

The first effect, super-Eddington nuclear fusion rates, results in the gradual turnover of the time-limited accretion curve in Figure 3, while the second effect comes into play on the right hand side of the dashed line separating the fully convective regime from the partially convective regime. The two effects ultimately limit the final mass of the star to  $\sim 10^6 M_{\odot}$ , even at the highest accretion rates. This can be found by solving for the lifetime of the star in the limit of a very large accretion rate. From equation (24), because  $r_{\text{trap}} \propto \dot{M}_{\text{acc}}$  the luminosity at which the nuclear fuel is burned in this limit is  $L_{\text{nuc}} \simeq L_{\text{Edd}} \frac{r_{\text{trap}}}{r_*}$ . Then, using our expressions for  $r_{\text{trap}}$  and  $r_*$  in equation (23), we find  $M_{\text{conv}} \simeq 0.9 M_*$ , which means that in this limit  $\simeq 90$  percent of the nuclear fuel contained in the star is available for fusion. Taking this as the energy budget, and integrating the luminosity over time, again using our expressions for  $r_{\text{trap}}$  and  $r_*$  in terms of  $M_*$  and  $\dot{M}_{\text{acc}}$ , we find the following for the lifetime of the star:

$$t_{\text{life}} \simeq 1.3 \times 10^6 \text{ yr} \left( \frac{\dot{M}_{\text{acc}}}{M_{\odot} \text{ yr}^{-1}} \right)^{-1}. \quad (25)$$

With this expression, the final stellar mass is  $M_* =$

<sup>12</sup> This statement assumes that nuclear burning commences when the star has a mass much lower than its final mass. However, we note that for Pop III stars with final masses of  $\sim 100 M_{\odot}$  nuclear burning may not begin until the star acquires a substantial fraction of its final mass (Omukai & Palla 2003); if so, the lifetime of the star will be much closer to the  $\sim 2$  Myr expected for  $\gtrsim 100 M_{\odot}$  Pop III stars of constant mass.

<sup>13</sup> In this event, the stellar photosphere also expands to  $r_{\text{trap}}$ , as previous authors have found when accretion rates trap the radiation from the star (Stahler et al. 1986; Omukai & Palla 2003). Since the internal temperatures of primordial protostars are lower than on the main sequence, their opacities are somewhat above those due to Thomson scattering alone. Consequently, their radii are found to swell to more than  $r_{\text{trap}}$  and perhaps terminate accretion, as discussed in Omukai & Palla (2003).

$\dot{M}_{\text{acc}} t_{\text{life}} \simeq 1.3 \times 10^6 M_{\odot}$ , independent of the accretion rate. This rough estimate is in good agreement with the asymptotic value of  $\simeq 1.5 \times 10^6 M_{\odot}$  shown in Fig. 3, for which we have integrated the stellar luminosity over the lifetime of the star starting from  $M_* = 0$ . For the constant accretion we have assumed in this calculation, there appears to be no way that a star can exceed this limiting mass, regardless of the rate at which it accretes material. After a certain time, its available nuclear fuel simply runs out and growth ends with the death of the star.

We note that ‘dark stars’, which are powered by dark matter annihilation, could grow to considerably higher masses than those powered by fusion (e.g. Freese et al. 2008). This is because the cooler surface temperatures of such stars exert much less radiative feedback on accretion and dark matter fuel may last for a much longer time than nuclear fuel. However, recent high resolution cosmological simulations show that primordial stars forming at the centers of dark matter halos may not remain there because of dynamical interactions, as required for the continual capture and annihilation of dark matter in their interiors (Stacy et al. 2011b; Greif et al. 2011). Therefore, it may be that the final masses of dark stars are not so different from those expected for standard primordial stars (see also Ripamonti et al. 2010). If, however, dark stars do grow to be more massive they would exhibit spectral properties distinct from those of solely fusion-powered supermassive Pop III stars (Zackrisson et al. 2010; Ilie et al. 2011), as we discuss next.

#### 4. OBSERVATIONAL SIGNATURES

As supermassive stars are intense sources of radiation that could be detected by current and future surveys, we now examine their observable signatures. The fact that radiative feedback in most cases cannot terminate accretion onto supermassive Pop III stars in collapsing protogalaxies implies that their H II regions will be confined deep in their host halos for most of their lives. It follows that their ionizing radiation is largely reprocessed into nebular emission instead of escaping the halo and reionizing the IGM. As noted in §2.2, because the accretion flow is optically thick to the Ly $\alpha$  photons, they cannot directly exit the halo and be observed. These photons are instead further reprocessed into Balmer series photons which do escape the H II region and halo and propagate into the IGM. Therefore, one likely signature of rapidly accreting, isolated supermassive Pop III stars in high-redshift protogalaxies is a strong Balmer line flux accompanied by a conspicuous lack of Ly $\alpha$  emission. A detailed radiative transfer calculation is necessary to quantitatively predict luminosities for all the Balmer lines in hydrogen, but we can place lower limits on the H $\alpha$  flux, which is expected to be the dominant line.

Following Schaerer (2002) and Raiter et al. (2010), we compute the luminosity  $L_{\text{H}\alpha}$  in H $\alpha$  as a function of  $Q_{\text{eff}}$  as discussed in §2.1. Relating this ionizing photon emission rate to stellar mass with equation 13 yields  $L_{\text{H}\alpha} \simeq 4 \times 10^{38} (M_*/100 M_{\odot}) \text{ erg s}^{-1}$ ; we again emphasize that this is a lower limit because we exclude reprocessing of Ly $\alpha$  into H $\alpha$ , which may dramatically boost H $\alpha$  luminosities

above those estimated here. The H $\alpha$  flux at redshift  $z$  is

$$f_{\text{H}\alpha} = \frac{L_{\text{H}\alpha}}{4\pi D_L^2} \sim 10^{-20} \text{ erg s}^{-1} \text{ cm}^{-2} \left( \frac{L_{\text{H}\alpha}}{10^{40} \text{ erg s}^{-1}} \right) \left( \frac{1+z}{10} \right)^{-2} \quad (26)$$

where  $D_L(z)$  is the luminosity distance to redshift  $z$ . We plot this flux as a function of stellar mass and redshift in Figure 4, with the arrows on the H $\alpha$  curves signifying lower limits.

The hard spectrum of ionizing radiation from hot primordial stars also creates an He III region from which a large luminosity in He II  $\lambda 1640$  emission is expected (Oh et al. 2001; Tumlinson et al. 2001; Bromm et al. 2001; Schaerer 2002; Johnson et al. 2009). Since the optical depth to this line is low, we also estimate how much of its flux exits the halo. For the large ionization rates and densities in our study, we can apply the standard model of Raiter et al. (2010) to compute the luminosity of this line, which we find to be  $L_{1640} \simeq 2 \times 10^{38} (M_*/100 M_{\odot}) \text{ erg s}^{-1}$ , where we again have used Table 1 of Bromm et al. (2001) for the number of He II-ionizing photons produced as a function of stellar mass. Then, replacing  $L_{\text{H}\alpha}$  with  $L_{1640}$  in equation 34, we derive the flux in the He II  $\lambda 1640$  line, which we plot with  $f_{\text{H}\alpha}$  in Figure 4 as a function of stellar mass and redshift.

Also shown in Figure 4 are detection limits for two instruments that will be on board the *James Webb Space Telescope (JWST)*: the Near-Infrared Spectrograph (NIRSpec) and the Mid Infrared Instrument (MIRI). The black dotted curves in Figure 4 denote the flux limits for  $3\sigma$  detection of the H $\alpha$  and He II  $\lambda 1640$  lines in an exposure time of  $10^4$  s at resolutions  $R = 1000$  for NIRSpec and  $R = 1200\text{-}2400$  for MIRI (Gardner et al. 2006).<sup>14</sup> Because ionizing photon rates vary linearly with stellar mass, so do recombination line fluxes. Consequently, only the more massive accreting primordial stars will be detectable by the *JWST*. Noting again that our H $\alpha$  line fluxes are lower limits, stars with masses  $\gtrsim 10^5 M_{\odot}$  may be detectable in H $\alpha$  out to  $z \gtrsim 10$ , while accreting stars with masses on the order of  $10^4 M_{\odot}$  could perhaps be detected out to somewhat lower redshift. Detection of the He II  $\lambda 1640$  line will only be possible from stars with masses of at least  $10^5 M_{\odot}$  for sufficiently long exposure times.

We note that the enhanced Balmer line emission from these objects may pose some difficulty to their identification as supermassive Pop III stars. As mentioned earlier, the large ratio of He II  $\lambda 1640$  flux to hydrogen recombination line flux in Ly $\alpha$  or H $\alpha$  is unique to Pop III stars. If, however, much of the Ly $\alpha$  emission is converted to H $\alpha$ , the drop in this ratio could mask the primordial nature of the star. That said, the absence of any Ly $\alpha$  emission would still likely reveal the central object to be an accreting supermassive star. Another attribute of rapidly accreting supermassive stars is strong continuum emission below the Lyman limit, which is the sum of the stellar continuum and the nebular continuum (e.g. Raiter et al. 2010); the latter would be substantial due to the exceptionally high densities expected in the H II regions of these stars. Indeed, it is possible that the sum of the stellar and nebular emission could be detected, for example, in the Deep-Wide

<sup>14</sup> JWST bandpass data can be found at [www.stsci.edu/jwst/science/sensitivity](http://www.stsci.edu/jwst/science/sensitivity).



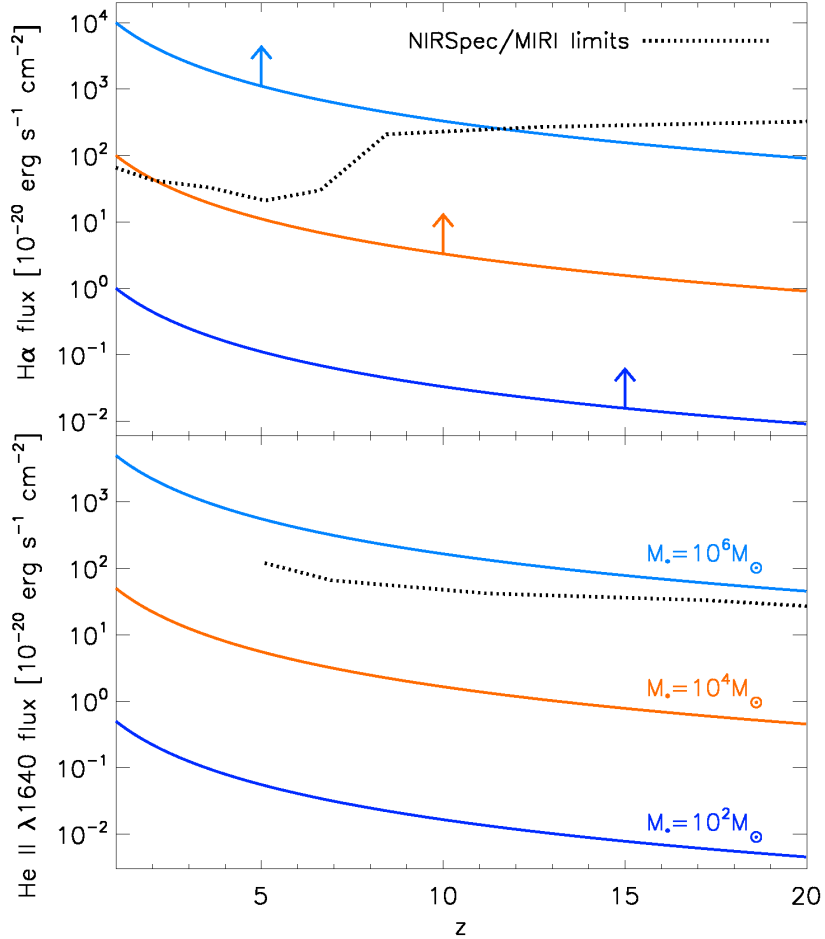


FIG. 4.— The flux in H $\alpha$  (top panel) and He II  $\lambda 1640$  (bottom panel) from accreting main sequence primordial stars, as a function of redshift  $z$ , for stellar masses of  $10^2$  (dark blue),  $10^4$  (red), and  $10^6 M_{\odot}$  (light blue). The dotted black lines show flux limits for  $3\sigma$  detection of these lines in  $10^4$  second exposures with the NIRSpect and MIRI instruments on the JWST, operating at resolutions  $R = 1000$  and  $R = 1200$ - $2400$ , respectively. NIRSpect operates at wavelengths of  $\simeq 1$  to  $5 \mu\text{m}$ , while MIRI covers the range from  $\simeq 5$  to  $28 \mu\text{m}$ . As discussed in § 4, as we have not accounted for the reprocessing of trapped Ly $\alpha$  photons into Balmer series photons (including H $\alpha$ ), the H $\alpha$  fluxes shown here are lower limits, as indicated by the arrows. While detection of H $\alpha$  from stars with masses of  $\gtrsim 10^4 M_{\odot}$  may be possible out to very high redshift (e.g.  $z \gtrsim 10$ ), only accreting primordial stars with masses of at least  $10^5 M_{\odot}$  are likely to be detectable in He II  $\lambda 1640$ .

Survey to be carried out with the Near-Infrared Camera (NIRCam) on the JWST.

An important obstacle to finding these objects is that their numbers could be small. As discussed by previous authors (Bromm & Loeb 2003; Dijkstra et al. 2004, 2008, see also Agarwal et al. in prep), supermassive stars cannot be so abundant that the black holes they create exceed observed limits on the black hole mass density and x-ray background. This suggests that finding the black holes may be easier than detecting their progenitors. First, they could accrete material for at least  $10^8$  yr and be luminous for far longer than the stars that created them. Second, future x-ray missions such as the *Joint Astrophysics Nascent Universe Satellite (JANUS)* (Roming 2008; Burrows et al. 2010), *LOBSTER* (Gorenstein 2011), *SVOM* (Götz et al. 2009), and the *Energetic X-ray Imaging Survey Telescope (EXIST)* (Grindlay 2005) will perform all sky surveys with far greater coverage than the JWST. However, if the nascent black hole does not have an accretion disk it may only emit

weakly in x-rays at birth (Fryer et al. 2001; Fryer & Heger 2011; Suwa & Ioka 2011, but see also Komissarov & Barkov 2010). If so, the SMBH seed does not become visible until it begins to accrete surrounding protogalactic gas (Haehnelt & Rees 1993; Kuhlen & Madau 2005; Li et al. 2007; Volonteri & Begelman 2010; Johnson et al. 2011).

Supermassive stars could also be detected if they explode as luminous supernovae. However, previous studies have concluded that  $\gtrsim 10^3 M_{\odot}$  Pop III stars collapse to black holes without an explosion (Fuller et al. 1986; Fryer & Heger 2011; Montero et al. 2011) (but see Ohkubo et al. 2006). At  $140 - 260 M_{\odot}$ , however, pair-instability supernovae occur (Heger et al. 2003) and may be observable by future missions such as the *JWST* (Wise & Abel 2005; Scannapieco et al. 2005; Weinmann & Lilly 2005; Joggerst & Whalen 2011; Kasen et al. 2011). Finally, we note that much of the continuum and line emission from rapidly accreting supermassive stars will appear in the near infrared background (NIRB) today. Although their contribution to the NIRB

may be small if they are rare, it could be detected by missions such as the *Cosmic Infrared Background Experiment* (CIBER; e.g. Bock et al. 2006), which is designed to find signatures of primordial galaxy formation at  $z \gtrsim 10$ .

## 5. DISCUSSION AND CONCLUSIONS

We find that the masses of the stellar seeds of SMBH forming from baryon collapse in early protogalaxies are primarily governed by their intense ionizing UV flux and their finite lifetimes. For spherically-symmetric accretion at constant rates  $\dot{M}_{\text{acc}} \lesssim 0.1 M_{\odot} \text{ yr}^{-1}$ , the maximum mass the star can reach is governed by radiative feedback and is  $M_* \simeq 10^3 (\dot{M}_{\text{acc}}/10^{-3} M_{\odot} \text{ yr}^{-1})^{\frac{8}{5}} M_{\odot}$ . At higher masses, the H II region breaks out to large radii and terminates accretion. We have verified that other forms of feedback, such as gas pressure, radiation pressure from trapped line emission, photodissociation of  $\text{H}^-$ , and scattering of Ly $\alpha$  photons are much less effective at slowing accretion (see §2.2 and the Appendix).

At accretion rates above  $\gtrsim 0.1 M_{\odot} \text{ yr}^{-1}$  the lifetime of the star, not radiative feedback, determines its final mass by limiting the time for which gas can accumulate on the star. Radiative feedback limits supermassive Pop III stars to final masses of  $\sim 3 \times 10^5 M_{\odot}$  and time-limited accretion limits them to  $\sim 10^6 M_{\odot}$ . Numerical simulations of protogalactic collapse find central infall rates of 0.1 - 1  $M_{\odot} \text{ yr}^{-1}$  (Wise et al. 2008; Shang et al. 2010; Johnson et al. 2011), suggesting that supermassive stars may typically approach the upper limit of  $\sim 10^6 M_{\odot}$ .

We caution that our analytical calculations do not account for all conceivable effects that could stem the growth of supermassive stars. For instance, McKee & Tan (2008) note that rotation of infalling gas leads to lower circumstellar densities and larger H II regions with greater radiative feedback (see also Hosokawa et al. 2011; Stacy et al. 2011a), implying lower final stellar masses. Our spherically-symmetric calculation excludes rotation, so the mass limits we find for a given accretion rate (Fig. 3) are upper limits. We do, however, find agreement with (Omukai & Inutsuka 2002), who performed a similar calculation, although they only considered the growth of stars up to  $\sim 10^3 M_{\odot}$ . Furthermore, we also note that the spherical symmetry and constant accretion in our models do not address accretion that is episodic or clumpy and self-shielded from ionizing radiation from the star (Whalen et al. 2008, 2010; Krumholz et al. 2009). These processes could cause accretion to proceed at lower time-averaged rates than those predicted here (but see Kuiper et al. 2011).

Another process that could truncate the growth of supermassive stars well before feedback or stellar lifetimes is the onset of a general relativistic instability in the core of the star that causes it to collapse when it becomes sufficiently massive (Chandrasekhar 1964). Such instabilities are predicted to set in once the star has grown to  $\sim 10^5 M_{\odot}$  (Iben 1963; Fowler 1964), but

stellar rotation could stabilize it against collapse up to much larger masses (Fowler 1966; Bisnovatyi-Kogan 1998; Baumgarte & Shapiro 1999). While our models ignore rotation, the accreting gas is likely to have some (e.g. Colgate et al. 2003); if so, the supermassive star will inherit the angular momentum of the gas from which it formed and perhaps bypass the general relativistic instability. Additional insight into the processes that limit the growth of supermassive stars will be gleaned from stellar evolution calculations accounting for the continual accretion of mass at high rates (Heger et al. in prep).

If supermassive stars formed and grew to masses of  $\gtrsim 10^5 M_{\odot}$  in the early universe, recombination emission from their H II regions may be bright enough to be detected by future missions such as the *JWST*. In particular, Ly $\alpha$  photons trapped in the accretion flow are reprocessed into Balmer series photons that could escape into the IGM. Consequently, the formation of these objects is accompanied by distinctive strong H $\alpha$  emission together with strong continuum and He II  $\lambda 1640$  emission, the latter arising from the hard spectrum of hot Pop III stars. However, their black holes may be easier to discover in observational surveys, given the small numbers and brief lifetimes of their progenitors. Indeed, these black holes may be the very ones that have already been found at the centers of massive galaxies and quasars at high redshifts.

Current numerical simulations of SMBH seed formation in early protogalaxies are now at an impasse because the formation of the hydrostatic supermassive protostar restricts Courant times to values that are too short to evolve central flows for even one dynamical time (but see Johnson et al. 2011 for an alternative approach using the sink particle technique). Our results suggest that in the early and intermediate stages of the growth of the star its evolution is essentially decoupled from flows on even slightly larger spatial scales. Consequently, it should now be possible to retreat from the extreme spatial resolutions previously applied to the protostar and evolve flows at the center of the galaxy over enough dynamical times to capture its structure at the time of the death of the star and breakout of x-rays from the BH seed into the IGM. Thus, it will soon be possible to witness the births of the first quasars in the universe with supercomputers.

## ACKNOWLEDGEMENTS

The authors would like to thank Stirling Colgate, Dave Collins, Alex Heger, Kevin Honnell, Sadegh Khochfar, Tsing-Wai Wong, and Hao Xu for helpful discussions. JJJ gratefully acknowledges the support of a LANL LDRD Director's Postdoctoral Fellowship at Los Alamos National Laboratory. DJW acknowledges support from the Bruce and Astrid McWilliams Center for Cosmology at CMU. Work at LANL was done under the auspices of the National Nuclear Security Administration of the U.S. Department of Energy at Los Alamos National Laboratory under Contract No. DE-AC52-06NA25396.

## REFERENCES

- Abel, T., Anninos, P., Zhang, Y., & Norman, M. L. 1997, *New A*, 2, 181  
 Abel, T., Bryan, G. L., & Norman, M. L. 2002, *Science*, 295, 93  
 Adams, T. F. 1972, *ApJ*, 174, 439  
 Alvarez, M. A., Bromm, V., & Shapiro, P. R. 2006, *ApJ*, 639, 621  
 Alvarez, M. A., Wise, J. H., & Abel, T. 2009, *ApJ*, 701, L133  
 Baumgarte, T. W. & Shapiro, S. L. 1999, *ApJ*, 526, 941  
 Begelman, M. C. 1978, *MNRAS*, 184, 53

- . 2010, *MNRAS*, 402, 673
- Begelman, M. C., Volonteri, M., & Rees, M. J. 2006, *MNRAS*, 370, 289
- Bisnovatyi-Kogan, G. S. 1998, *ApJ*, 497, 559
- Bock, J., Battle, J., Cooray, A., Kawada, M., Keating, B., Lange, A., Lee, D.-H., Matsumoto, T., Matsuura, S., Pak, S., Renbarger, T., Sullivan, I., Tsumura, K., Wada, T., & Watabe, T. 2006, *New A Rev.*, 50, 215
- Braun, E. & Dekel, A. 1989, *ApJ*, 345, 31
- Bromm, V., Coppi, P. S., & Larson, R. B. 2002, *ApJ*, 564, 23
- Bromm, V., Kudritzki, R. P., & Loeb, A. 2001, *ApJ*, 552, 464
- Bromm, V. & Loeb, A. 2003, *ApJ*, 596, 34
- Burrows, D. N., Roming, P. W. A., Fox, D. B., Herter, T. L., Falcone, A., Bilén, S., Nousek, J. A., & Kennea, J. A. 2010, in Presented at the Society of Photo-Optical Instrumentation Engineers (SPIE) Conference, Vol. 7732, Society of Photo-Optical Instrumentation Engineers (SPIE) Conference Series
- Cen, R. 1992, *ApJS*, 78, 341
- Chandrasekhar, S. 1964, *ApJ*, 140, 417
- Chuzhoy, L., Kuhlen, M., & Shapiro, P. R. 2007, *ApJ*, 665, L85
- Clark, P. C., Glover, S. C. O., Smith, R. J., Greif, T. H., Klessen, R. S., & Bromm, V. 2011, *Science*, 331, 1040
- Colgate, S. A., Cen, R., Li, H., Currier, N., & Warren, M. S. 2003, *ApJ*, 598, L7
- Devecchi, B. & Volonteri, M. 2009, *ApJ*, 694, 302
- Dijkstra, M., Haiman, Z., & Loeb, A. 2004, *ApJ*, 613, 646
- Dijkstra, M., Haiman, Z., Mesinger, A., & Wyithe, J. S. B. 2008, *MNRAS*, 391, 1961
- Dijkstra, M. & Wyithe, J. S. B. 2010, *MNRAS*, 408, 352
- Djorgovski, S. G., Volonteri, M., Springel, V., Bromm, V., & Meylan, G. 2008, in The Eleventh Marcel Grossmann Meeting On Recent Developments in Theoretical and Experimental General Relativity, Gravitation and Relativistic Field Theories, ed. H. Kleiner, R. T. Jantzen, & R. Ruffini, 340–367
- Dotan, C., Rossi, E. M., & Shaviv, N. J. 2011, *MNRAS*, 417, 3035
- Elitzur, M. & Ferland, G. J. 1986, *ApJ*, 305, 35
- Fan, X., Strauss, M. A., Schneider, D. P., Becker, R. H., White, R. L., Haiman, Z., Gregg, M., Pentericci, L., Grebel, E. K., Narayanan, V. K., Loh, Y., Richards, G. T., Gunn, J. E., Lupton, R. H., Knapp, G. R., Ivezić, Ž., Brandt, W. N., Collinge, M., Hao, L., Harbeck, D., Prada, F., Schaye, J., Strateva, I., Zakamska, N., Anderson, S., Brinkmann, J., Bahcall, N. A., Lamb, D. Q., Okamura, S., Szalay, A., & York, D. G. 2003, *AJ*, 125, 1649
- Fowler, W. A. 1964, *Reviews of Modern Physics*, 36, 545
- . 1966, *ApJ*, 144, 180
- Freese, K., Spolyar, D., & Aguirre, A. 2008, *J. Cosmology Astropart. Phys.*, 11, 14
- Fryer, C. L. & Heger, A. 2011, *Astronomische Nachrichten*, 332, 408
- Fryer, C. L., Woosley, S. E., & Heger, A. 2001, *ApJ*, 550, 372
- Fuller, G. M., Woosley, S. E., & Weaver, T. A. 1986, *ApJ*, 307, 675
- Gorenstein, P. 2011, in Society of Photo-Optical Instrumentation Engineers (SPIE) Conference Series, Vol. 8147, Society of Photo-Optical Instrumentation Engineers (SPIE) Conference Series
- Götz, D., Paul, J., Basa, S., Wei, J., Zhang, S. N., Atteia, J.-L., Barret, D., Cordier, B., Claret, A., Deng, J., Fan, X., Hu, J. Y., Huang, M., Mandrou, P., Mereghetti, S., Qiu, Y., & Wu, B. 2009, in American Institute of Physics Conference Series, Vol. 1133, American Institute of Physics Conference Series, ed. C. Meegan, C. Kouveliotou, & N. Gehrels, 25–30
- Greif, T. H., Springel, V., White, S. D. M., Glover, S. C. O., Clark, P. C., Smith, R. J., Klessen, R. S., & Bromm, V. 2011, *ApJ*, 737, 75
- Grindlay, J. E. 2005, *New A Rev.*, 49, 436
- Haehnelt, M. G. & Rees, M. J. 1993, *MNRAS*, 263, 168
- Heger, A., Fryer, C. L., Woosley, S. E., Langer, N., & Hartmann, D. H. 2003, *ApJ*, 591, 288
- Hosokawa, T., Omukai, K., Yoshida, N., & Yorke, H. W. 2011, *ArXiv e-prints*
- Hummer, D. G. & Storey, P. J. 1987, *MNRAS*, 224, 801
- Iben, Jr., I. 1963, *ApJ*, 138, 1090
- Ilie, C., Freese, K., Valluri, M., Iliev, I. T., & Shapiro, P. 2011, *ArXiv e-prints*
- Inayoshi, K. & Omukai, K. 2011, *MNRAS*, 416, 2748
- Jeon, M., Pawlik, A. H., Greif, T. H., Glover, S. C. O., Bromm, V., Milosavljević, M., & Klessen, R. S. 2011, *ArXiv e-prints*
- Joggerst, C. C. & Whalen, D. J. 2011, *ApJ*, 728, 129
- Johnson, J. L. & Bromm, V. 2007, *MNRAS*, 374, 1557
- Johnson, J. L., Greif, T. H., Bromm, V., Klessen, R. S., & Ippolito, J. 2009, *MNRAS*, 399, 37
- Johnson, J. L. & Khochfar, S. 2011, *ArXiv e-prints*
- Johnson, J. L., Khochfar, S., Greif, T. H., & Durier, F. 2011, *MNRAS*, 410, 919
- Kasen, D., Woosley, S. E., & Heger, A. 2011, *ArXiv e-prints*
- Kitayama, T., Yoshida, N., Susa, H., & Umemura, M. 2004, *ApJ*, 613, 631
- Koushiappas, S. M., Bullock, J. S., & Dekel, A. 2004, *MNRAS*, 354, 292
- Krumholz, M. R., Klein, R. I., McKee, C. F., Offner, S. S. R., & Cunningham, A. J. 2009, *Science*, 323, 754
- Kuhlen, M. & Madau, P. 2005, *MNRAS*, 363, 1069
- Kuiper, R., Klahr, H., Beuther, H., & Henning, T. 2011, *ArXiv e-prints*
- Li, Y. 2011, *ArXiv e-prints*
- Li, Y., Hernquist, L., Robertson, B., Cox, T. J., Hopkins, P. F., Springel, V., Gao, L., Di Matteo, T., Zentner, A. R., Jenkins, A., & Yoshida, N. 2007, *ApJ*, 665, 187
- Lodato, G. & Natarajan, P. 2006, *MNRAS*, 371, 1813
- Madau, P. & Rees, M. J. 2001, *ApJ*, 551, L27
- McKee, C. F. & Tan, J. C. 2008, *ApJ*, 681, 771
- Milosavljević, M., Bromm, V., Couch, S. M., & Oh, S. P. 2009, *ApJ*, 698, 766
- Montero, P. J., Janka, H.-T., & Mueller, E. 2011, *ArXiv e-prints*
- Mortlock, D. J., Warren, S. J., Venemans, B. P., Patel, M., Hewett, P. C., McMahon, R. G., Simpson, C., Theuns, T., González-Solares, E. A., Adamson, A., Dye, S., Hambly, N. C., Hirst, P., Irwin, M. J., Kuiper, E., Lawrence, A., & Röttgering, H. J. A. 2011, *Nature*, 474, 616
- Nakamura, F. & Umemura, M. 2001, *ApJ*, 548, 19
- Oh, S. P. & Haiman, Z. 2002, *ApJ*, 569, 558
- Oh, S. P., Haiman, Z., & Rees, M. J. 2001, *ApJ*, 553, 73
- Ohkubo, T., Nomoto, K., Umeda, H., Yoshida, N., & Tsuruta, S. 2009, *ApJ*, 706, 1184
- Ohkubo, T., Umeda, H., Maeda, K., Nomoto, K., Suzuki, T., Tsuruta, S., & Rees, M. J. 2006, *ApJ*, 645, 1352
- Omukai, K. & Inutsuka, S.-i. 2002, *MNRAS*, 332, 59
- Omukai, K. & Palla, F. 2001, *ApJ*, 561, L55
- . 2003, *ApJ*, 589, 677
- Omukai, K., Schneider, R., & Haiman, Z. 2008, *ApJ*, 686, 801
- O’Shea, B. W. & Norman, M. L. 2007, *ApJ*, 654, 66
- Osterbrock, D. E. & Ferland, G. J. 2006, *Astrophysics of gaseous nebulae and active galactic nuclei*, ed. Osterbrock, D. E. & Ferland, G. J.
- Park, K. & Ricotti, M. 2011, *ApJ*, 739, 2
- Pelupessy, F. I., Di Matteo, T., & Ciardi, B. 2007, *ApJ*, 665, 107
- Raiter, A., Schaerer, D., & Fosbury, R. A. E. 2010, *A&A*, 523, A64
- Regan, J. A. & Haehnelt, M. G. 2009, *MNRAS*, 396, 343
- Ripamonti, E., Iocco, F., Ferrara, A., Schneider, R., Bressan, A., & Marigo, P. 2010, *MNRAS*, 406, 2605
- Roming, P. 2008, in COSPAR, Plenary Meeting, Vol. 37, 37th COSPAR Scientific Assembly, 2645–+
- Scannapieco, E., Madau, P., Woosley, S., Heger, A., & Ferrara, A. 2005, *ApJ*, 633, 1031
- Schaerer, D. 2002, *A&A*, 382, 28
- Schleicher, D. R. G., Spaans, M., & Glover, S. C. O. 2010, *ApJ*, 712, L69
- Sethi, S., Haiman, Z., & Pandey, K. 2010, *ApJ*, 721, 615
- Shang, C., Bryan, G. L., & Haiman, Z. 2010, *MNRAS*, 402, 1249
- Shibata, M. & Shapiro, S. L. 2002, *ApJ*, 572, L39
- Spaans, M. & Silk, J. 2006, *ApJ*, 652, 902
- Spitzer, L. 1978, *Physical processes in the interstellar medium*, ed. Spitzer, L.
- Stacy, A., Greif, T. H., & Bromm, V. 2010, *MNRAS*, 403, 45
- . 2011a, *ArXiv e-prints*
- Stacy, A., Pawlik, A. H., Bromm, V., & Loeb, A. 2011b, *ArXiv e-prints*
- Stahler, S. W., Palla, F., & Salpeter, E. E. 1986, *ApJ*, 302, 590
- Suwa, Y. & Ioka, K. 2011, *ApJ*, 726, 107
- Tanaka, T. & Haiman, Z. 2009, *ApJ*, 696, 1798
- Tumlinson, J., Giroux, M. L., & Shull, J. M. 2001, *ApJ*, 550, L1
- Turk, M. J., Abel, T., & O’Shea, B. 2009, *Science*, 325, 601
- Volonteri, M. 2010, *A&A Rev.*, 18, 279
- Volonteri, M. & Begelman, M. C. 2010, *MNRAS*, 409, 1022
- Weinmann, S. M. & Lilly, S. J. 2005, *ApJ*, 624, 526
- Whalen, D., Abel, T., & Norman, M. L. 2004, *ApJ*, 610, 14
- Whalen, D., Hueckstaedt, R. M., & McConkie, T. O. 2010, *ApJ*, 712, 101
- Whalen, D., O’Shea, B. W., Smidt, J., & Norman, M. L. 2008, *ApJ*, 679, 925
- Willott, C. J., McLure, R. J., & Jarvis, M. J. 2003, *ApJ*, 587, L15
- Wise, J. H. & Abel, T. 2005, *ApJ*, 629, 615
- Wise, J. H., Turk, M. J., & Abel, T. 2008, *ApJ*, 682, 745
- Wishart, A. W. 1979, *MNRAS*, 187, 59P
- Wolcott-Green, J., Haiman, Z., & Bryan, G. L. 2011, *MNRAS*, 418, 838
- Wyithe, S. & Loeb, A. 2011, *ArXiv e-prints*
- Yoshida, N., Omukai, K., & Hernquist, L. 2008, *Science*, 321, 669
- Zackrisson, E., Scott, P., Rydberg, C.-E., Iocco, F., Edvardsson, B., Östlin, G., Sivertsson, S., Zitring, A., Broadhurst, T., & Gondolo, P. 2010, *ApJ*, 717, 257

## APPENDIX

## NEGLECTED FEEDBACK PROCESSES

Here, we discuss several processes which have a negligible impact on our estimate of the the final maximum stellar mass given by equation 15.

*He II Photoionization*

To assess the relative importance of He II photoionization in slowing the accretion flow in the He III region, we follow the argument in Section 2.1 for He I photoionization. For the ratio of He II photoionization pressure to H I photoionization pressure, we have

$$\frac{p_{\text{HeII}}}{p_{\text{HI}}} \simeq \frac{n_{\text{He}}}{n_{\text{H}}} \frac{h\nu_{\text{HeII}}}{h\nu_{\text{HI}}} \frac{\alpha_{\text{B,HeII}}}{\alpha_{\text{B,HI}}} \simeq 1.1, \quad (\text{A1})$$

where we have taken it that  $h\nu_{\text{HeII}}/h\nu_{\text{HI}} \simeq 54.4 \text{ eV} / 29 \text{ eV} \simeq 1.8$ , and that  $\alpha_{\text{B,HeII}}/\alpha_{\text{B,HI}} \simeq 6.4$  (Osterbrock & Ferland 2006). Therefore, within the He III region, the radiation pressures due to He II and H I photoionizations are comparable. This is convenient because in the He III region it is recombination emission from He II, not stellar photons, which largely keeps hydrogen photoionized (Osterbrock & Ferland 2006). Therefore, while this diffuse recombination emission does not transfer appreciable outward momentum to the gas, the stellar photons that ionize He II transfer roughly the same momentum to the gas that they would in ionizing H I. As a consequence, solving in detail for the pressure due to He II photoionization would result in an almost identical solution to the one we have found by just treating the H II region.

*H<sup>-</sup> Photodetachment*

In order for very high accretion rates onto a supermassive star in a primordial protogalaxy to be realized, the H<sub>2</sub> fraction in the accreting protogalactic gas must be very low (Bromm & Loeb 2003; Lodato & Natarajan 2006; Spaans & Silk 2006; Omukai et al. 2008; Wise et al. 2008). Indeed, the  $\gtrsim 10^4 \text{ K}$  virial temperatures at the centers of  $10^7 - 10^8 M_{\odot}$  halos heavily suppress H<sub>2</sub> fractions, so it is a good approximation to take it that the opacity due to absorption of photons by H<sub>2</sub> is also low. However, this does not imply that H<sup>-</sup> fractions are negligible because it forms from reactants whose abundances are not suppressed by H<sub>2</sub>-dissociating backgrounds or high virial temperatures:



where  $\gamma$  denotes the emission of a photon. In principle, the absorption of photons with energies  $\geq 0.75 \text{ eV}$  by photodetachment of H<sup>-</sup> could be an important channel by which momentum can be imparted to inflow. To determine the rate at which momentum that could be transferred to the gas, it suffices to estimate the equilibrium rate of H<sup>-</sup> formation, since this is also the rate at which H<sup>-</sup> will be destroyed and momentum will be acquired by the gas (see Abel et al. 1997; Chuzhoy et al. 2007). Using the density profiles from our calculations, which assume that the gas falls toward the star at the free-fall velocity above  $r_{\text{HII}}$  (Fig. 2), we have  $n(r) \lesssim 10^{12} (r/r_{\text{HII}})^{-\frac{3}{2}} \text{ cm}^{-3}$ . Numerical simulations of protogalactic collapse predict central free electron fractions  $f_e \sim 10^{-4}$  (e. g. Shang et al. 2010). With these as upper limits along with the rate coefficient  $k_{\text{H}^{-}}$  for H<sup>-</sup> formation, integration over the density profile of the halo yields the H<sup>-</sup> formation rate  $Q_{\text{H}^{-}}$  outside the H II region:

$$Q_{\text{H}^{-}} \lesssim k_{\text{H}^{-}} \int_{r_{\text{HII}}}^{r_{\text{outer}}} 4\pi r^2 f_e n^2 dr \simeq 10^{44} \text{ s}^{-1}, \quad (\text{A3})$$

where  $k_{\text{H}^{-}} \sim 10^{-14} \text{ cm}^3 \text{ s}^{-1}$  (Wishart 1979; Abel et al. 1997). We assume that hydrogen is predominantly neutral outside the H II region and neglect the small H<sup>-</sup> fractions that may form in the H II region. Finally, to ensure that we have found a strong upper limit, we integrate this profile out to  $r_{\text{outer}} = 10^{21} \text{ cm}$ , which is approximately the virial radius of the atomically-cooled halos at high redshift that host the supermassive stars we are studying. Even allowing for the high average photon energy for photodetachment  $h\nu_{\text{H}^{-}} \sim 10 \text{ eV}$  for supermassive Pop III stars, the maximum momentum that could be transferred to the gas per unit time is

$$\frac{h\nu_{\text{H}^{-}} Q_{\text{H}^{-}}}{c} \lesssim 10^{22} \text{ g cm s}^{-2}. \quad (\text{A4})$$

This is orders of magnitude smaller than the momentum of the accretion flow in equation 18, so H<sup>-</sup> destruction does not contribute to radiative feedback.

*Radiation Pressure from Trapped Ly $\alpha$  and Balmer Series Lines*

In Section 2.2, we raised the possibility that Ly $\alpha$  photons may slow down accretion by scattering from neutral atoms at the edge of the H II region. While we showed that this is unlikely to alter the flow, mostly because Ly $\alpha$  photons are confined to  $r_{\text{Ly}\alpha}$ , radiation pressure due to nebular emission lines in optically thick gas may be sufficient to reduce accretion. As also mentioned in Section 2.2, trapped Ly $\alpha$  photons are largely converted to Balmer series photons, in some cases after being destroyed by absorption in excited hydrogen or helium (Osterbrock & Ferland 2006). These Balmer photons can then propagate outward and efficiently cool the gas. The high temperatures, densities, and Ly $\alpha$  photons trapped in the H II region cause a large fraction of the hydrogen atoms to be excited to the  $n = 2$  state there. From this

state, either collisions or absorptions will further excite the atoms, which often later decay by emitting a Balmer series photon.

To evaluate the degree to which radiation pressure from trapped line photons alters the dynamics of accretion, we first estimate the optical depth to Balmer photons both inside and outside the H II region. Within  $r_{\text{HII}}$ , the density of neutral hydrogen atoms can be estimated from equation 21 and assuming that  $n \propto r^{-2}$ , as implied by the nearly constant velocity profile of the gas in the H II region (Fig. 2). The neutral hydrogen column density  $N_{\text{H}}$  through the H II region is then

$$\begin{aligned} N_{\text{H}}(< r_{\text{HII}}) &\simeq \int_{r_*}^{r_{\text{HII}}} f_{\text{HI}}(r) n(r) dr \\ &= f_{\text{HI}}(r_{\text{HII}}) n(r_{\text{HII}}) \frac{r_{\text{HII}}^2}{r_*} \simeq 10^{17} \text{ cm}^{-2}, \end{aligned} \quad (\text{A5})$$

which, from the scaling in the second equation, can be shown to have only a weak dependence on the stellar mass for  $M_* = 10^2 - 10^6 M_{\odot}$  for our solutions to the minimum accretion rate. The cross sections for absorption of Balmer series photons by H in the  $n = 2$  state are 19, 3.5, and  $1.3 \times 10^{-17} \text{ cm}^2$  for H $\alpha$ , H $\beta$ , and H $\gamma$ , respectively. The higher energy Balmer series cross sections are all below these values. With these cross sections and  $N_{\text{H}}(< r_{\text{HII}})$ , we can express the optical depth through the H II region solely as a function of the relative populations  $N_2/N_1$  of the  $n = 1$  and  $n = 2$  levels of neutral hydrogen in the H II region. We find that even for  $N_2/N_1$  as high as  $\sim 0.05$ , the H II region is optically thin to all Balmer series photons, while the largest optical depth possible for H $\alpha$  is  $\tau_{\text{H}\alpha} \simeq 20$ . However, this is still far below the optical depth for Ly $\alpha$  photons, and Balmer series photons will eventually leak out of the H II region, although in some cases only after a number of scatterings. Therefore, while Ly $\alpha$  photons in general will not escape the H II region, Balmer series photons will escape and allow the gas to radiatively cool, as we noted in Section 2.2.

Next, we consider the optical depth to Balmer series lines outside the H II region. In this region, we set  $f_{\text{HI}} = 1$  and adopt a free-fall density profile  $n \propto r^{-\frac{3}{2}}$  for the gas, as in Section 2.1. The neutral hydrogen column density beyond  $r_{\text{HII}}$  is then

$$\begin{aligned} N_{\text{H}}(> r_{\text{HII}}) &\simeq \int_{r_{\text{HII}}}^{\infty} n(r) dr \\ &= 2n(r_{\text{HII}})r_{\text{HII}} \simeq 10^{24} \text{ cm}^{-2}, \end{aligned} \quad (\text{A6})$$

which again is not strongly dependent on stellar mass.

Because the gas outside the H II region is well below the critical density at which excited levels in hydrogen would be populated and kept in equilibrium by collisions (and because Ly $\alpha$  photons are mostly trapped in the H II region and cannot excite neutral hydrogen beyond  $r_{\text{HII}}$ ), the relative population of the  $n = 2$  level of hydrogen is expected to be very small. In this case, Schleicher et al. (2010) find that in general  $N_2/N_1 \lesssim 10^{-10}$ . With this as an upper limit and the cross sections for Balmer series photon absorption above, we find that the optical depths to Balmer series lines are  $\tau_{\text{H}\alpha} \sim 4 \times 10^{-2}$ ,  $\tau_{\text{H}\beta} \sim 8 \times 10^{-3}$ , and  $\tau_{\text{H}\gamma} \sim 3 \times 10^{-3}$ . At such low optical depths, Balmer series photons will propagate largely unimpeded through the inflow and, most likely, exit the halo with minimal effect on accretion. As these photons also move freely through the intergalactic medium (IGM), accreting supermassive stars probably have a distinctive observational signature, as we discussed in § 4.

Thus, because outside the H II region the optical depth to Balmer series photons is small and Ly $\alpha$  photons cannot propagate across the H II region boundary, we conclude that radiation pressure due to trapped emission lines will not be appreciable beyond  $r_{\text{HII}}$ . However, it may be that this pressure is substantial within the H II region. To estimate its magnitude, we compare it to the ram pressure of the accretion flow. For the latter, we have

$$\begin{aligned} P_{\text{ram}} &= n\mu m_{\text{H}}v^2 \\ &\simeq 50 \left( \frac{\dot{M}_{\text{acc}}}{M_{\odot} \text{ yr}^{-1}} \right) \left( \frac{r}{10^{15} \text{ cm}} \right)^{-2} \left( \frac{v}{100 \text{ km s}^{-1}} \right) \text{ dyn cm}^{-2}, \end{aligned} \quad (\text{A7})$$

where we have used equation 1 to express  $n$  in terms of  $v$  and  $\dot{M}_{\text{acc}}$ . We use the prescription of Braun & Dekel (1989) for the radiation pressure (see also Elitzur & Ferland 1986):

$$P_{\text{line}} = \left( \frac{4\pi}{9c} \right) \left( \frac{2h\nu_{\text{tran}}^3}{c^2} \right) \frac{N_{i+1}}{N_i} \Delta\nu_{\text{tran}}, \quad (\text{A8})$$

where  $N_{i+1}/N_i$  is the ratio of the upper and lower level populations for the given transition, whose frequency is  $\nu_{\text{tran}}$ . The line width  $\Delta\nu_{\text{tran}} \sim 2 \times 10^{11} (T/10^4 \text{ K})^{\frac{1}{2}} (\ln \tau)^{\frac{1}{2}} \text{ s}^{-1}$ , where  $\tau$  is the optical depth of the line.

Assuming optical depths  $\tau_{\text{Ly}\alpha} = 10^4$  and  $\tau_{\text{Balmer}} = 20$ , both of which are rough upper limits in the H II region, and  $N_{i+1}/N_i = 1$  in both cases, we find strong upper limits of  $\sim 6 \text{ dyn cm}^{-2}$  and  $2 \times 10^{-2} \text{ dyn cm}^{-2}$  for the Ly $\alpha$  and Balmer line radiation pressures, respectively. Comparing these pressures to  $P_{\text{ram}}$  at  $r_{\text{HII}}$ , which is a lower limit for the H II region due to its strong dependence on  $r$  in equation A7, we find that it is always at least a factor of  $\sim 4$  larger than radiation pressure from optically thick lines. Therefore, lines will not play a large role in slowing accretion in the H II region.

### Gas Pressure

Because infall is highly supersonic, gas pressure cannot decelerate the gas (Omukai & Inutsuka 2002). We have verified that this holds even when a gas pressure term is included in the equation of motion. We find that only for extremely

high sound speeds corresponding to temperatures of at least  $10^6$  K would gas pressure begin to impact the dynamics of the accretion flow. However, temperatures this high are not found in numerical simulations of protogalactic collapse (Wise et al. 2008; Regan & Haehnelt 2009; Shang et al. 2010; Johnson et al. 2011) or in H II regions because the Balmer thermostat limits ionized gas temperatures to at most a few  $\times 10^4$  K.

#### *Accretion Luminosity*

Our conclusions regarding the maximum mass of the supermassive star rest on the assumption that the critical accretion rate for a given stellar mass (equation 12) separates two regimes: below this rate, accretion is suppressed by radiative feedback and above this rate accretion proceeds. As shown in Section 2.1, it is clear that accretion is prevented for inflow rates below the critical rate because the ionization front breaks out to infinity and photoionization pressure halts infall at all radii. For accretion rates above the critical rate, the flow will arrive at the star with a velocity  $v(r_*) > 0$ . This implies that the accreting material will have some kinetic energy that must be dissipated at the stellar surface, some portion of which will be radiation. This radiation could slow accretion within the H II region by electron scattering or photoionizations.

Let us assume that all of the kinetic energy of the flow is converted to radiation that propagates outward on impact with the star at some velocity  $v(r_*)$ . The luminosity thus generated is

$$L_{\text{acc}} = \frac{\dot{M}_{\text{acc}} v^2}{2}, \quad (\text{A9})$$

which yields a total momentum in photons of  $L_{\text{acc}}/c = \dot{M}_{\text{acc}} v^2/2c$ . Comparing this to the momentum of the infalling gas,  $\dot{M}_{\text{acc}} v$ , we see that the momentum in the accretion luminosity is a factor  $v/2c$  lower than that of the gas. Therefore, accretion radiation cannot halt the flow in the steady-state approximation. However, bouts of massive accretion could in principle generate enough radiation to slow infall at larger radii where gas has a lower momentum, like the episodic accretion onto black holes in the early universe discussed by Milosavljević et al. (2009).

We note that an additional effect of accretion at very high rates (much higher than those in equation 12) is the trapping of radiation by electron scattering or other sources of opacity in the flow (e.g. Begelman 1978, 2010; Wyithe & Loeb 2011). As discussed by Omukai & Palla (2003, see also Stahler et al. 1986) in the context of primordial protostellar accretion, radiation trapping can lead to rapid expansion of the stellar photosphere that halts the growth of the star. We note, however, that such expansion also causes the effective temperature of the star to fall with the increase in surface area of the photosphere<sup>15</sup>, which in turn leads to a softening of the emitted radiation and a lower ionizing photon emission rate  $Q$ . This, and the fact that accretion rates greater than those in equation 12 result in smaller H II regions, suggests that the flow cannot be stopped, at least not by photoionization pressure.

<sup>15</sup> At constant luminosity, the effective temperature at the stellar photosphere scales as  $T_{\text{eff}} \propto r_*^{-\frac{1}{2}}$